



OBSERVATIONAL RESULTS HINTING AT THE COUPLING OF THE THERMOSPHERE WITH THE IONOSPHERE/MAGNETOSPHERE SYSTEM AND WITH THE MIDDLE ATMOSPHERE

E. Illés-Almár,* I. Almár* and P. Bencze**

* Konkoly Observatory, H-1525 Budapest Box 67, Hungary

** Geodetic and Geophysical Research Institute, H-9401 Sopron Box 5,
Hungary

ABSTRACT

Total density data based on CACTUS microaccelerometer measurements have been analysed between 220 and 700 km altitudes at low latitudes in the time interval 1975–79. Instantaneous residual density values with respect to atmospheric models for quiet as well as for disturbed days have been investigated as a function of local solar time (LST). It has been found that the density residuals present conspicuous increases of the variance in several LST intervals as well as a general broadening which can be in connection with various coupling mechanisms between the thermosphere and the ionosphere/magnetosphere on the one hand, and the middle atmosphere on the other. An attempt is made to select those mechanisms responsible for the observed features.

INTRODUCTION

The investigation of the geomagnetic activity effect (which is the density increase in connection with geomagnetic storms) in the neutral upper atmosphere is continued based on CACTUS microaccelerometer measurements of the French CASTOR satellite /1/. Our improved geomagnetic term – using Dst /2/ instead of Kp /2/ as parameter of the activity – is added to a MSIS'86 model /3/ value calculated with Kp=0 (hMSIS model /4/). Residuals with respect to this hMSIS model were analysed: local humps in the diurnal course were interpreted as consequences of local energy depositions connected to the ring current heating /5/.

In the first part of the present paper the height profile of the heating rate – derived from the measured geomagnetic term – has been compared to the profile of heating by precipitating particles. In the second part the general broadening or scatter of the residuals has been analysed to clarify whether gravity waves may play role in this phenomenon as it has been suggested earlier /6/.

DATA AND METHOD

The observational material /1/ and the method /7/ used were described in previous papers. Thermospheric density data for 220–700 km height interval and for the time interval 1975–79 have been separated according to the level of geomagnetic activity. On the basis of the Dst curve 29 time intervals of ~100 days total length were selected as "quiet time data" where the Dst curve remained near its maximum value at least for several days. The first four days of 41 geomagnetic storms with rather steep descending branches have been selected as "disturbed periods" also on the basis of the Dst curve.

The measured $\Delta\rho$ geomagnetic term has been defined as the excess density with respect to the corresponding MSIS'86 (with Kp=0) value: $\Delta\rho = \rho^{CAC} - \rho^{MSIS'86(Kp=0)}$. It has been demonstrated earlier that this measured geomagnetic term can be best described – at least at these altitudes near the equator – as a function of Dst in the form: $\Delta\rho = a \cdot Dst^2 + b \cdot Dst + c$ where a, b and c are height dependent functions. Based on these a, b and c values determined for different altitudes the height dependence of

the heating rate has been calculated and compared to the corresponding function belonging to particle precipitation (Fig. 1). The period with low solar activity (P1 curve) from 27 June 1975 to 11 February 1978 is characterized by $\overline{S_{10.7}} = 81.7$, $\overline{Dst} = -18$, $\overline{T_{\infty}} = 750$ K parameters, the period with higher solar activity (P3 curve) from 30 August 1978 to 21 January 1979 by $\overline{S_{10.7}} = 162.6$, $\overline{Dst} = -32.8$, $\overline{T_{\infty}} = 1050$ K parameters respectively. ($S_{10.7}$ is the solar 10.7 cm radiation flux in $10^{-22} \text{Wm}^{-2}\text{Hz}^{-1} / 2$, T_{∞} is the exospheric temperature.)

In order to investigate the relation of the effect to the middle atmosphere — in quiet and in disturbed periods separately — the hMSIS residuals $f-1 = (\rho_{CAC} - \rho_{hMSIS}) / \rho_{hMSIS}$ and the scatter computed from deviations from the $f-1$ mean values has been analysed in the 220–700 km height interval. The diurnal course of the scatter has been derived from a 3-hours average value of $f-1$ at different heights. The height dependence of the scatter has been investigated as well at different geomagnetic latitudes and seasons. In this case height intervals are unequal in order to assure the necessary number of measurements at every height. Summer has been defined as July, August and September in the Northern, and January, February and March in the Southern hemisphere and vice versa.

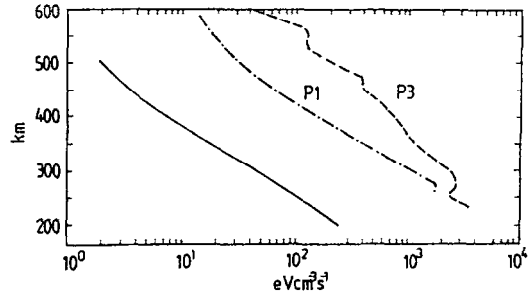


Fig.1. Height variation of the heating rate based on the measured geomagnetic term for low (P1) and higher (P3) solar activity. The height variation of the heating rate of atmospheric disturbances originating from the auroral zone is indicated by heavy line.

DISCUSSION

Coupling of the Thermosphere with the Ionosphere/Magnetosphere

Considering the coupling between the thermosphere and the ionosphere/magnetosphere system, we assumed and tried to prove in our earlier papers /5,8/ that the excess density and the bulk of the geomagnetic activity term in density at low latitudes can be due to the heating caused by the energy deposition of precipitating energetic neutral atoms and ions originating from the ring current. The height variation of the energy deposition by precipitating energetic particles differs from that of the solar electromagnetic radiation /9/ and atmospheric disturbances spreading from the auroral zones. Our results indicate that the height variation of the heating rate determined from the measured geomagnetic term displays a curve similar to the height variation of the heating rate by particles (Fig. 1). As comparison,

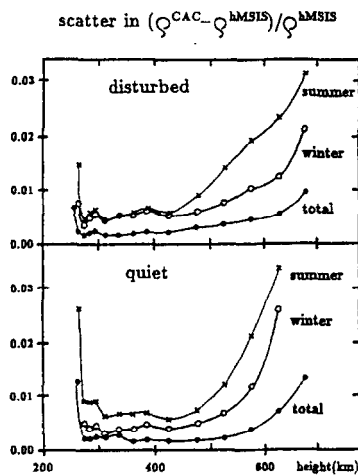


Fig.2. Height variation of the scatter in the residuals for entire years (total) and in different seasons for geomagnetically quiet and disturbed periods as well.

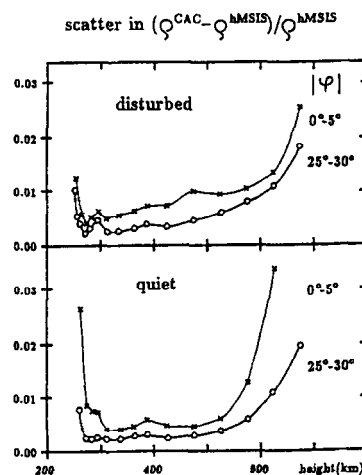


Fig.3. Altitude variation of the scatter in the residuals separated according to geomagnetic latitudes. The scatter is diminishing with increasing geomagnetic latitude, hinting at an equatorial source.

the modelled heating rate of atmospheric disturbances for $T_{\infty} = 750$ K at low latitudes originating from the auroral zones is also plotted by heavy line.

The density of the neutral upper atmosphere is lower during a solar activity minimum, therefore the energy deposition begins at lower heights and the maximum is also shifted to lower heights. This is demonstrated by the height variation of the heating rate deduced from the measurements. The P1 curve indicates a more or less continuous increase of the heating rate with decreasing height, which seems to reach its maximum at a

height of 270 km. The slope at the upper part of the curve (above 500 km) is larger than at lower heights corresponding to the energy deposition of O particles during low solar activity /10/. The shape of the P3 curve is more complicated. Three secondary maxima can be observed on this curve dividing it into three parts. If we suppose that the energy deposition producing the heating rate comes from neutral and charged particles, the change of the slope at different parts of the P3 curve can be interpreted on the basis of the following considerations. The loss of energy of the particles decreases while the penetration depth increases with increasing energy. Beginning from above the upper part has the smallest slope and thus could correspond to the energy deposition by low energy particles – oxygen atoms or ions. The secondary maximum at 550 km indicates the possibility of this assumption. The second section of the curve has a somewhat larger dip, but it can also be attributed to a group of low energy particles with energies somewhat higher than those producing the upper part of the curve. The secondary maximum appearing at about 470 km is in favour of this supposition. Another small secondary maximum may occur at 380 km (corresponding to a change in the slope of the curve), but it is not as definite as the previous maxima. Finally the third part of the curve is characterised by the largest slope and it ends in a well developed secondary maximum at a height of 270 km. Taking into account the above mentioned three or four changes in the course of the curve, they may correspond from top to bottom to the maximum energy loss of particles with increasing energy and increasing penetration depth (having energies less than some keV).

$$\frac{(\varphi^{CAC} - \varphi^{hMSIS})}{\varphi^{hMSIS}}$$

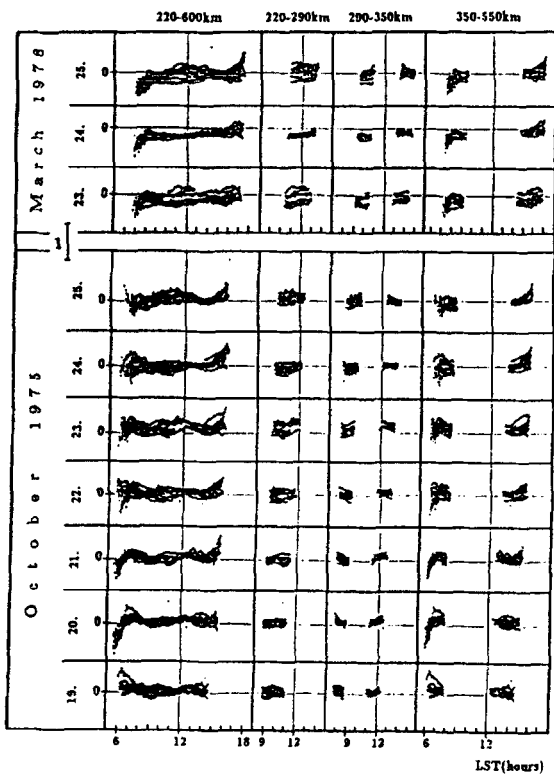


Fig.5. The hMSIS model residuals clearly demonstrate a day-to-day variability in their scattering in two quiet intervals. The plot is separated according to height as well in order to point out height intervals with increased scatter.

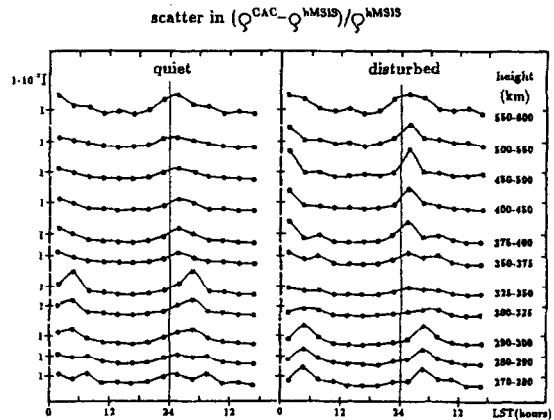


Fig.4. Diurnal variation of the scatter in the residuals. The phase of the maximum decreases with increasing height.

Coupling of the thermosphere with the middle atmosphere

It has been assumed in /6/ that the even scatter found in the residuals might be due to atmospheric gravity waves. In the middle atmosphere their characteristic variations are:

- height variation of the amplitude and phase of the gravity waves,
- a seasonal variation in activity with a maximum at low latitudes in the summer and a smaller one in winter /11/,
- a large day-to-day variability.

Regarding our results first the height dependence is investigated (Fig. 2 and 3). It is interesting that the mean scatter first steeply decreases with increasing height, but then remains constant in a long height interval, while at greater altitudes it begins to increase again – independently whether it has been separated according to some parameter or not. Fig. 2 presents the height variation of the scatter computed for different seasons. There are greater values in summer than in winter, and both are larger than the yearly

average (total). The effect is visible both in geomagnetically quiet and in disturbed periods and at all heights. It is interesting that the difference between the summer and winter months is larger in geomagnetically quiet periods. Fig.3 presents the height variation of the scatter computed for different geomagnetic latitudes. It decreases with increasing geomagnetic latitude both in geomagnetically quiet and in disturbed periods. This can hint at an equatorial origin. Fig. 4 presents the diurnal variation of the scatter. A definite maximum appears at night the phase of which is clearly shifted with increasing height to earlier hours that is the phase decreases with increasing height. Besides the sources in the middle atmosphere, the trace of which can be detected below 300 km, there are another sources of the fluctuations that can be recognized at about 300 km in geomagnetically quiet periods and at about 400 km in geomagnetically disturbed periods. Nevertheless the time of occurrence of this maximum is strange. It coincides with the time of the occurrence of the early morning disturbance zone at high latitudes /12/, but in the case of the second source it is more probable that the scatter originates in the F region due to sudden heating, which can be related to particle precipitation /5,8/. The day-to-day variability is illustrated in Fig.5 and 6. In Fig.5 the momentan residuals themselves are plotted as a function of LST for consecutive days, also indicating the height ranges of the column. In Fig.6 the day-to-day variability of the daily average scatter in residuals is plotted for different height ranges: there is a change with altitude. Thus as it is demonstrated in Fig. 2,3,4,5 and 6 the scatter represented by the curves has similar characteristics to that of gravity waves in the middle atmosphere.

CONCLUSIONS

The heating rate based on the measured geomagnetic term of the neutral upper atmosphere and attributed to particle precipitation at low latitudes indicates its uniform increase with decreasing height at low solar activity. In the case of higher solar activity some secondary maxima appear on the heating rate profile, changing the slope of the variation as well. The phenomenon might be interpreted by the loss of energy of neutral and charged particles (e.g. O, O⁺) having different energy less than some keV. The characteristics of the scatter of the residuals, the height variation and the phase shift with increasing height, the seasonal variation, the day-to-day variability make it possible to interpret these fluctuations as internal gravity waves. Their sources can be located partly in the middle atmosphere, partly in the height range 300–400 km. Both sources can be related to some form of geomagnetic activity.

REFERENCES

1. F.Barlier, J.Bouttes, M.Delattre, A.Olivero, P.Contensou, *Compt.Rend.Sc. Paris*, 281B, 145 (1975).
2. NSSDC Handbook of Correlative Data, ed.: J.H. King, NASA, GSFC (1971).
3. *Adv. Space Res.* 8, 5-6 (1988).
4. I.Almár, E.Illés-Almár, A.Horváth, J.Kelemen, D.V.Bisikalo, T.V.Kasimenko, 30th COSPAR Meeting, Hamburg, Paper C.1-014 (1994).
5. P.Bencze, I.Almár, E.Illés-Almár, *Adv. Space Res.* 13, (1)303-306 (1993).
6. E.Illés-Almár, II. IAGA Buenos Aires, session 3.15+5.5, IAGA Bull. No.55, p.23 (1993).
7. I.Almár, E.Illés-Almár, A.Horváth, Z.Kolláth, D.V.Bisikalo, T.V.Kasimenko, *Adv. Space Res.* 12 (6)313-316 (1992).
8. P.Bencze, I.Almár, E.Illés-Almár, 29th COSPAR Meeting, Washington, paper C.5-M.3.06 (1992).
9. M.R.Torr, D.G.Torr and R.Roble, in: *The Physical Basis of the Ionosphere in the Solar-Terrestrial System*, Hatford House, London (1980).
10. M.R.Torr, D.G.Torr, R.G.Roble and E.C.Ridley, *J. Geophys. Res.* 87, 5290 (1982).
11. I.Hirota, in: *Dynamics of the Middle Atmosphere*, Terra, Tokyo, D.Reidel, Dordrecht, (1984).
12. G.W.Pröls, M.Roemer and J.W.Slowey, *Adv. Space Res.* 8, (5)215-(5)216 (1988).

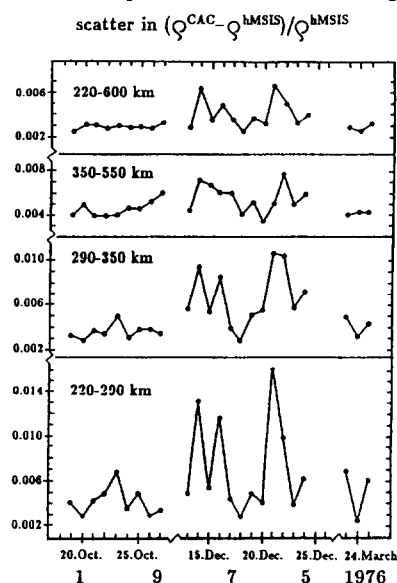


Fig.6. Daily scatter values of the residuals in different height intervals, with an additional third quiet period added to Fig. 5.